vered into the ESR spectral cavity, and data collection was commenced. Once the sample was in place, it was not moved. A plot of signal intensity for a selected peak versus the square root of microwave power was carried out at 10 K, to establish microwave powers at which saturation would not occur. We typically used a ≤500-μW microwave power setting. All spectra were obtained with an identical number of scans and with identical spectrometer power settings. Reproducibility of signal intensities was checked by raising and lowering temperature in the region of 10–50 K, once the annealed sample was produced.

After spectra were obtained, double integration was carried out using standard Bruker software. Plots of double integration intensity versus corrected temperature were analyzed by nonlinear least-squares methods.

For method 3 in the variable-temperature apparatus, the procedure was identical with that described above, save that the samples were frozen and degassed under vacuum in 3-mm o.d. quartz tubes, placed in the cavity of the E-9 ESR spectrometer, cooled to 60–65 K, photolyzed by ca. 1800 pulses from a XeCl excimer laser (Lambda Physik EMG 103 MSC, λ = 308 nm, pulse power at sample ca. 50 mJ), and then examined spectroscopically as described in the previous two paragraphs.

Acknowledgment. We acknowledge partial financial assistance from the Exxon Education Foundation and the University of Massachusetts Graduate School in this work. We acknowledge helpful assistance from APD Cryogenics Corp. (Mr. Ravi Bains and Ms. Elizabeth Hammond) in the design of our cryogenic Displex ESR experiments. We also acknowledge pleasant and stimulating correspondence with Prof. Hiizu Iwamura and are grateful for his providing us with information on the results of his studies on related dinitrenes in advance of publication.

Photophysics and Photochemistry of 22π and 26π Acetylene–Cumulene Porphyrinoids

Daniel O. Mártire,[†] Norbert Jux,[‡] Pedro F. Aramendía,[§] R. Martín Negri,[§] Johann Lex,[‡] Silvia E. Braslavsky,[†] Kurt Schaffner,*[,†] and Emanuel Vogel*[,‡]

Contribution from the Max-Planck-Institut für Strahlenchemie, D-4330 Mülheim an der Ruhr, Federal Republic of Germany, Institut für Organische Chemie, Universität Köln, D-5000 Köln 41, Federal Republic of Germany, and Facultad de Ciencias Exactas y Naturales, Departamento de Química Inorgánica, Analítica y Química Física, Universidad de Buenos Aires, 1428 Buenos Aires, Argentina. *Received May 19, 1992*

Abstract: The aromatic 26π acetylene–cumulene porphyrinoid **8** has been synthesized by a reaction sequence involving reductive carbonyl coupling of the dialdehyde **12** utilizing low-valent titanium in the crucial step. Like its lower 22π homologs **6** and **7**, the new tetrapyrrolic macrocycle **8** is centrosymmetric in the crystal and has a practically planar ring framework. The photophysical and photochemical properties of **6–8** have been studied and compared to those of the related 18π porphycene **5**. The absorption spectrum of **8** has the most red-shifted and intensified visible bands (ϵ_{max} = 119 600 at 889 nm in dichloromethane) of this particular series of $(4n + 2)\pi$ porphyrinoids. None of the compounds exhibit any photoreactivity. The photophysical properties were determined by a combination of techniques, including steady-state thermal lensing, flash photolysis, laser-induced optoacoustic spectroscopy (LIOAS), and steady-state and time-resolved NIR spectroscopy. The 22π and 26π porphyrinoids do not phosphoresce. The triplet energy (E_T) of **7** was therefore measured by way of reversible energy transfer to oxygen yielding singlet molecular oxygen, $O_2(^1\Delta_g)$, indirect detection by LIOAS of the increase in triplet yield induced by $O_2(^3\Sigma_g^-)$-enhanced S → T intersystem crossing afforded the E_T of **6**, and an upper limit of E_T could be obtained by energy-transfer experiments from $O_2(^1\Delta_g)$ to **8**. The quantum yields of fluorescence, triplet formation, and the E_T values dropped significantly on going from **5** to **6–8** (all measurements at room temperature). The triplet energies of **6**, **7**, and **8** are all below the energy of $O_2(^1\Delta_g)$. Compound **7**, with the highest E_T of the three, produces $O_2(^1\Delta_g)$ with a quantum yield of Φ_Δ = 0.06 through a reversible energy-transfer mechanism. Although this value is about six times smaller than Φ_Δ of **5**, the phototherapeutic activities of both **5** and **7** toward tumors in mice are comparable. The Φ_Δ values for **6** and **8** are lower than 10^{-3}; hence, these porphyrinoids do not function as photodynamic sensitizers.

Introduction

Porphycene (**1**; Scheme I), isomeric to porphyrin from which it is derived formally by a mere reshuffling of the pyrrole and methine moieties, is a novel tetrapyrrolic macrocycle commanding interest from many points of view.[1] Numerous investigations[2] of **1** bear out the anticipated close relationship of this molecule to porphyrin, but they also reveal noticeable differences between the two isomers, qualifying **1** as a porphyrinoid in its own right.

The finding that porphycenes and metalloporphycenes are porphyrin-like pigments—and thus promise practical applications in various domains—was an incentive to us to devise expanded porphycenes expected to match or complement the expanded porphyrins[3] and related macrocycles[4] in their physical and chemical properties. In order to be endowed with aromatic stability, the new porphyrinoids envisioned must contain main conjugation pathways involving $(4n + 2)$ π electrons with $n > 4$.[5]

A clue as to how porphycenes might be translated into variants with an expanded structure meeting the electronic prerequisites is provided by the bonding in the intriguing acetylene–cumulene [4n + 2]dehydroannulenes.[6] As exemplified by the prototypical

Scheme I. Expansion of Porphycene (**1**) by Acetylene–Cumulene Structural Units to **2** and **3** and Juxtaposition of These Homologs with 1,2,8,9-Tetradehydro[14]annulene (**4**)

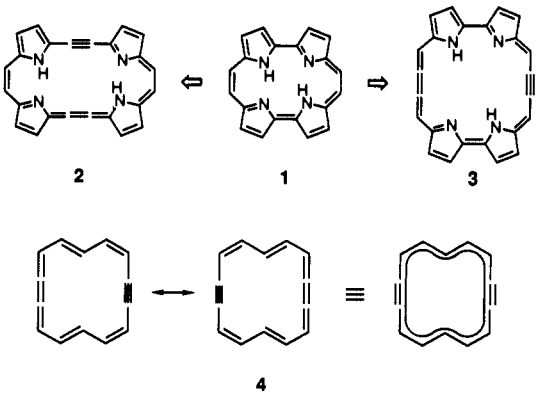

[†] Max-Planck-Institut für Strahlenchemie, Mülheim a. d. Ruhr.
[‡] Universität Köln.
[§] Universidad de Buenos Aires.

0002-7863/92/1514-9969$03.00/0

Chart I. The 22π and 26π Porphyrinoids **6**, **7**, and **8** under Study in Comparison with the 18π 2,7,12,17-Tetrapropylporphycene (**5**)

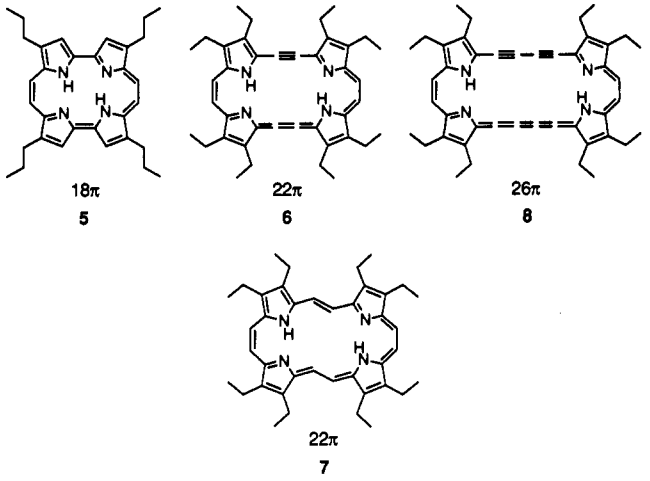

1,2,8,9-tetradehydro[14]annulene (**4**),[7] these annulenes possess one or more pairs of linear $C_{sp^2}(C_{sp}C_{sp})_nC_{sp^2}$ structural units (in this case $n = 1$) and are best described by equivalent Kekulé resonance structures having acetylene and cumulene bonds (Scheme I).

The most obvious expanded porphycenes featuring acetylene–cumulene structural units that come to mind are the isomeric porphyrinoids **2** and **3**. Both compounds contain 22π main conjugation pathways embedded into planar ring skeletons. The concept of employing acetylene–cumulene units in the development of novel porphyrinoids has recently proved viable by the synthesis of the type-**2** octaethyl derivative **6**[8,9] (Chart I). In line with expectation **6** had provided access to yet another porphyrinoid of topical interest, viz., octaethyl[22]porphyrin-(2.2.2.2) which, existing as the di-trans isomer **7**, bears a closer structural relationship to porphycene than to porphyrin.[10] While the synthesis of **3** has not yet been achieved, the even more expanded porphycene **8**, a 26π homolog of **1**, has now been synthesized in a straightforward manner.

Scheme II[a]

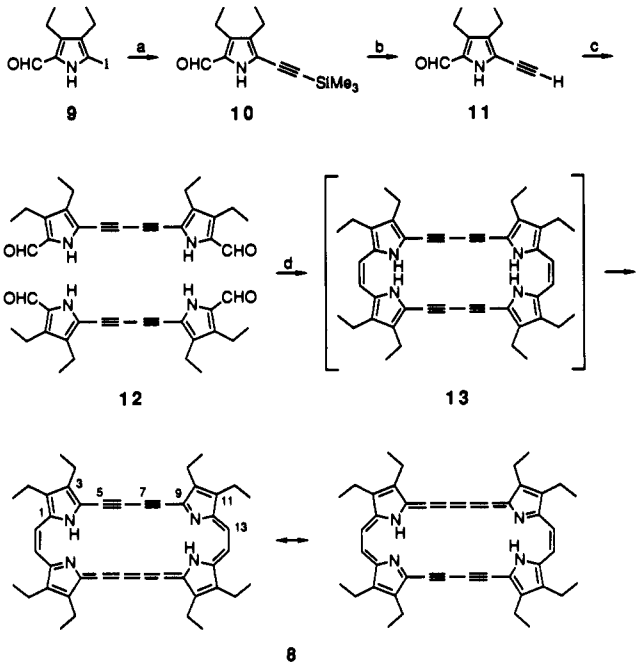

[a] (a) $HC{\equiv}CSiMe_3$, $(PPh_3)_2PdCl_2$, CuI, $HNEt_2$, 50 °C, 30 min, 90%; (b) NaOH, $MeOH/H_2O$, 25 °C, 30 min, 90%; (c) $ClCH_2COC-H_3$, $(PPh_3)_4Pd$, NEt_3, C_6H_6, 25 °C, 16 h, 75%; (d) $TiCl_4$, Zn, CuCl, THF, reflux, 20 min, 9%.

The availability of **6**, **7**, and **8** invited a detailed comparative investigation of these compounds using **5** as a reference. As part of this project, we here report on the particularly relevant excited-state properties of this set of porphyrinoids.

The Synthesis of the 26π Acetylene–Cumulene Porphyrinoid 8

A general method of porphycene synthesis, based on the reductive coupling of 5,5′-diformyl- or 5,5′-diacylbipyrroles with low-valent titanium agents[11] (generated preferentially from titanium tetrachloride and zinc/copper(I) chloride in tetrahydrofuran[12]), has been developed at the Cologne laboratory.[1a,8,10] Attesting to the aromatic stability of porphycenes, the primary product of the coupling reaction, viz., the respective *N,N′*-dihydroporphycene, cannot be isolated (except in special cases[13]) since it undergoes dehydrogenation to product even when oxygen is excluded rigorously. The spontaneous dehydrogenation of *N,N′*-dihydroporphycenes together with the ease with which large-membered rings are formed in reductive carbonyl couplings[14] offered the chance that the novel 22π acetylene–cumulene porphyrinoid **6** could be synthesized from bis(3,4-diethyl-5-formyl-2-pyrryl)acetylene. As reported recently,[8] **6** is obtained indeed when the latter compound is subjected to reductive coupling.

The interesting properties of the acetylene–cumulene 22π porphyrinoid **6** and of its hydrogenation product **7** led to attempts to synthesize also the 26π porphyrinoid **8**, the next higher aromatic homolog of **6**. In this case, the strategy of basing the crucial step of the synthesis on reductive carbonyl coupling required a ready access to the diacetylenic dialdehyde **12** (Scheme II). By use

(1) (a) Vogel, E.; Köcher, M.; Schmickler, H.; Lex, J. *Angew. Chem., Int. Ed. Engl.* **1986**, *25*, 257–258. (b) Vogel, E. *Pure Appl. Chem.* **1990**, *62*, 557–564. (c) Vogel, E.; Köcher, M.; Lex, J.; Ermer, O. *Isr. J. Chem.* **1989**, *29*, 257–266.

(2) (a) Aramendía, P. F.; Redmond, R. W.; Nonell, S.; Schuster, W.; Braslavsky, S. E.; Schaffner, K.; Vogel, E. *Photochem. Photobiol.* **1986**, *44*, 555–559. (b) Redmond, R. W.; Valduga, G.; Nonell, S.; Braslavsky, S. E.; Schaffner, K.; Vogel, E.; Pramod, K.; Köcher, M. *J. Photochem. Photobiol. B* **1989**, *3*, 193–207. (c) Ofir, H.; Regev, A.; Levanon, H.; Vogel, E.; Köcher, M.; Balci, M. *J. Phys. Chem.* **1987**, *91*, 2686–2688. (d) Schlüpmann, J.; Huber, M.; Toporowicz, M.; Plato, M.; Köcher, M.; Vogel, E.; Levanon, H.; Möbius, K. *J. Am. Chem. Soc.* **1990**, *112*, 6463–6471. (e) Waluk, J.; Müller, M.; Swiderek, P.; Köcher, M.; Vogel, E.; Hohlneicher, G.; Michl, J. *J. Am. Chem. Soc.* **1991**, *113*, 5511–5527. (f) Gael, V. I.; Kuz'mitskii, V. A.; Solov'ev, K. N. *Zh. Prikl. Spektrosk.* **1991**, *55*, 282–290.

(3) *N,N′,N″,N‴*-Tetramethyl[26]porphyrin-(3.3.3.3) dication: Gosmann, M.; Franck, B. *Angew. Chem., Int. Ed. Engl.* **1986**, *25*, 1100–1101. *N,N′,N″,N‴*-Tetramethyl[34]porphyrin-(5.5.5.5) dication: Knübel, G.; Franck, B. *Angew. Chem., Int. Ed. Engl.* **1988**, *27*, 1170–1172. [22]Porphyrin-(1.3.1.3): König, H.; Eickmeier, C.; Möller, M.; Rodewald, U.; Franck, B. *Angew. Chem., Int. Ed. Engl.* **1990**, *29*, 1393–1395 and references therein. Platyrins: Weaver, O. G.; LeGoff, E. *J. Org. Chem.* **1987**, *52*, 710–711 and references therein.

(4) Sapphyrins: Sessler, J. L.; Cyr, M. J.; Burrell, A. K. *Synlett* **1991**, 127–134 and references therein. Pentaphyrins: Rexhausen, H.; Gossauer, A. *J. Chem. Soc., Chem. Commun.* **1983**, 275. Texaphyrins: Sessler, J. L.; Murai, T.; Hemmi, G. *Inorg. Chem.* **1989**, *28*, 3390–3393 and references therein. Rubyrin: Sessler, J. L.; Morishima, T.; Lynch, V. *Angew. Chem., Int. Ed. Engl.* **1991**, *30*, 977. For a review on expanded porphyrins, see: Sessler, J. L.; Burrel, A. K. *Top. Curr. Chem.* **1991**, *161*, 177–273.

(5) Janson, T. R.; Katz, J. J. In *The Porphyrins*; Dolphin, D., Ed.; Academic Press: New York, 1979; Vol. IV, Part B, pp 1–59.

(6) Sondheimer, F. *Pure Appl. Chem.* **1963**, *7*, 363–388 and references therein.

(7) Batley, N. A.; Mason, R. *Proc. Chem. Soc.* **1963**, 180.

(8) Jux, N.; Koch, P.; Schmickler, H.; Lex, J.; Vogel, E. *Angew. Chem., Int. Ed. Engl.* **1990**, *29*, 1385–1387.

(9) Tetra-n-propyl (**5**) and octaethyl substitution (**6–8**) provides for better solubility.

(10) Vogel, E.; Jux, N.; Rodriguez-Val, E.; Lex, J.; Schmickler, H. *Angew. Chem., Int. Ed. Engl.* **1990**, *29*, 1387–1390.

(11) McMurry, J. E. *Chem. Rev.* **1989**, *89*, 1513–1524. Lenoir, D. *Synthesis* **1989**, 883–897.

(12) The in situ preparation of a zinc/copper pair ensures a constant quality of the reducing agent.

(13) Vogel, E.; Grigat, I.; Köcher, M.; Lex, J. *Angew. Chem., Int. Ed. Engl.* **1989**, *28*, 1655–1657.

(14) Kato, N.; Nakanishi, K.; Takeshita, H. *Bull. Chem. Soc. Jpn.* **1986**, *59*, 1109–1123. Brudermüller, M.; Musso, H. *Angew. Chem., Int. Ed. Engl.* **1988**, *27*, 298–299. McMurry, J. E.; Rico, J. G.; Shih, Y. *Tetrahedron Lett.* **1989**, *30*, 1173–1176.

Table I. Photophysical Properties of **5–8** in Benzene at Room Temperature[a]

	5[b]	**6**	**7**	**8**
E_S (kJ·mol^{-1})	188 ± 5	153 ± 8	149 ± 8	133 ± 8
τ_S (ns)[c]	9.76[d]	1.0	2.0	nd[e]
Φ_f	0.38[d,f]	0.12 ± 0.08[g]	0.08 ± 0.08[g]	<0.1[h]
Φ_{ic}^0[i]	0.34 ± 0.05	0.91 ± 0.10	0.79 ± 0.10	nd
τ_T (μs)[c,j]	270[f]	90 ± 20	115 ± 28	15.8 ± 2.7
Φ_T^0	0.4[f]	0.16 ± 0.02	0.22 ± 0.01	<2 × 10^{-3}
E_T (kJ·mol^{-1})	124[f]	78 ± 4	91 ± 1	<82
$\Delta\epsilon_{T-T}$ (M^{-1} cm^{-1})[k]	2.1 × 10^4[f]	(2.7 ± 0.7) × 10^4	(5.0 ± 0.7) × 10^4	2.4 × 10^4
Φ_Δ	0.36[d,f]	<10^{-3}[l]	0.06[m]	<10^{-3}[l]

[a] The values of Φ_T^0, E_T, $\Delta\epsilon_{T-T}$, and Φ_Δ were determined by different combinations of methods for each of the three compounds **6**, **7**, and **8** (cf. Determination of Triplet Energies, Quantum Yields of S → T Intersystem Crossing, and Triplet Absorption Coefficients). [b] Literature values of **5**, measured in toluene, added for comparison. [c] The lifetimes τ_S and τ_T were measured in degassed solutions. [d] Reference 2a. [e] Not determined, nd. [f] Reference 1b. [g] The large errors result from the determination of relatively small values by difference formation. [h] The ratio of the energy-weighted slopes for sample and reference gave $\Phi_f = -0.06 \pm 0.1$. Since the thermal lensing method is limited to determine Φ_f values of <0.15,[53] the negative value reflects an upper limit for Φ_f of 0.1 or less. [i] Calculated from $[E^{exc}(\alpha - 1) + E_S]/E_S$, with values obtained in the absence of O_2. Compare these Φ_{ic}^0 values with those obtained alternatively from $1 - (\Phi_f + \Phi_T^0) = 0.22 \pm 0.16$ (**5**), 0.72 ± 0.09 (**6**), and 0.70 ± 0.09 (**7**). [j] T–T spectrum recorded at λ^{exc} = 395 nm (**5**) and 640 nm (**6–8**). [k] λ^{obs} = 395 nm for **5** and 480, 500, and 520 nm for **6**, **7**, and **8**, respectively. [l] Formation of $O_2(^1\Delta_g)$ not observed. [m] Average of the values $\Phi_\Delta = 0.07 \pm 0.01$ (λ^{exc} = 355 nm) and 0.05 ± 0.02 (λ^{exc} = 666 nm).

of modern palladium chemistry,[15] the known 3,4-diethyl-5-formyl-2-iodopyrrole (**9**)[8] that has already served as the starting material for the preparation of **6** was converted straightforwardly into **12**. The iodoaldehyde **9** on reaction with (trimethylsilyl)-acetylene, catalyzed by bis(triphenylphosphine)palladium(II) chloride/copper(I) iodide, underwent ethynylation[16] to give **10** (90% yield) which was desilylated with sodium hydroxide in methanol affording the terminal acetylene **11** (90% yield). A tetrakis(triphenylphosphine)palladium(0)/copper(I) iodide catalyst in the presence of chloroacetone and triethylamine[17] was then employed to oxidatively couple **11** with formation of the diacetylenic dialdehyde **12** (75% yield). Finally, reductive coupling of **12** with titanium tetrachloride and zinc/copper(I) chloride led to **13**, which, as anticipated, was subject to spontaneous dehydrogenation to yield the desired 26π porphyrinoid **8**. After purification **8** was obtained as air-stable bluish green rhombs with metallic luster (9% yield).

The structure and aromaticity of the 26π acetylene–cumulene porphyrinoid **8** are already evident from the spectra of the new tetrapyrrolic macrocycle. The ^{1}H NMR spectrum, for which no temperature dependence has been so far observed from −100 to 20 °C, consists of a singlet at δ 10.08 (H-13), two quartets at δ 4.63 (H-2a) and 4.22 (H-3a), two triplets at δ 2.41 (H-2b) and 2.09 (H-3b), and a broadened signal at δ 2.04 (NH). This spectrum is almost superimposable on that of **6** and thus shows that the two compounds are homologous expanded porphycenes possessing strong NH···N hydrogen bonds. In accord herewith, the ^{13}C NMR spectrum of **8**, while exhibiting the same pattern as that of **6** regarding the resonances of the carbon atoms of the two porphycene halves, contains two resonances for the acetylene–cumulene type carbon atoms (δ 95.84 and 94.82, as compared to δ 105.75 in **6**). In the UV–visible spectrum of **8**, the close electronic relationship of **8** to **6**—and to 2,7,12,17-tetrapropylporphycene (**5**)—manifests itself impressively. As illustrated by Figure 1, the spectrum of **8** has almost the same appearance as that of **6** but has experienced a bathochromic shift that is consistent with the increased length of the main conjugation pathway (26π instead of 22π electron system). The mass spectrum (EI, 70 eV) shows the molecular ion (m/z 630) as the base peak and, as an additional peak, the doubly charged molecular ion (m/z 315, 5%). The presence of strong NH···N hydrogen bonds, indicated by the position of the resonance of the NH protons in the ^{1}H NMR spectrum at relatively low field, is further supported in the IR spectrum by the absence of a band in the region 3360–3300 cm^{-1}, typical for the NH stretching vibration. An intense absorption

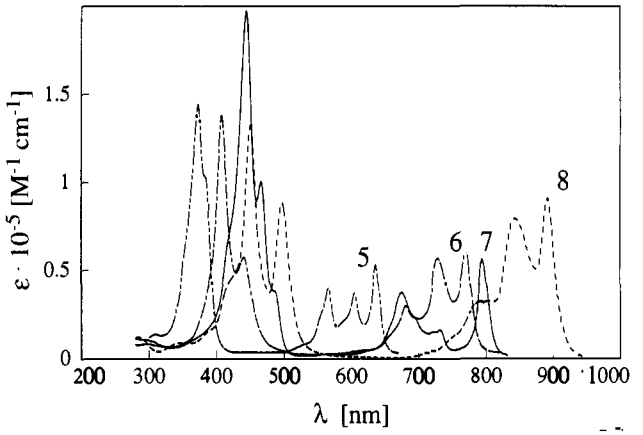

Figure 1. UV–visible ground-state absorption spectra of compound **5** (18π; ——·——), **6** (22π; ——), **7** (22π; —), and **8** (26π; – – –) in air-saturated benzene solutions.

at 2022 cm^{-1} corresponds to the asymmetric $C_{sp}C_{sp}$ stretching vibration.

The conclusions derived from the spectral results for the 26π acetylene–cumulene porphycene **8** are corroborated by a single-crystal X-ray analysis of the compound since this shows **8** to be centrosymmetric in the crystal lattice and to possess a practically planar ring framework. According to the symmetry observed, the $C_{sp^2}(C_{sp})_4C_{sp^2}$ structural units on opposite sides are equivalent. Hence, it is justified to formulate **8** as a resonance hybrid. The crystal structure of **8** reveals that this porphyrinoid excellently agrees with **6** regarding length and size of corresponding bonds and angles, respectively, a finding that underscores the homologous nature of the two compounds. The NH hydrogen atoms in **8**, like those in **6** but unlike those in **1**, are not disordered, so that an assignment to specific nitrogen atoms (which must be the N atoms in diagonal positions owing to symmetry) is possible.

The Photophysical and Photochemical Study: Results

Measurements of the photophysical properties of compounds absorbing in the far-red region are often not trivial in view of the difficulty associated with the choice of appropriate references in this spectral region. Moreover, since none of the 22π and 26π porphyrinoids exhibit any phosphorescence which could be assigned unambiguously,[18] a judicious choice of the methods to determine triplet energies had to be made.

Ground-State Absorption and Fluorescence Spectroscopy. The UV–visible ground-state absorption spectra of compounds **5–8** are shown in Figure 1. With the spectral range of the fluorescence of **6–8** extending to the NIR region, the emission spectra of these compounds had to be recorded with a steady-state IR emission spectrometer equipped with a germanium diode detector. The normalized uncorrected fluorescence spectra of air-saturated

(15) Tsuji, J. *Synthesis with Palladium Compounds*; Springer: Berlin, 1980.
(16) Dieck, H. A.; Heck, F. R. *J. Organomet. Chem.* **1975**, *93*, 259–263. Sonogashira, K.; Tohda, Y.; Hagihara, N. *Tetrahedron Lett.* **1975**, 4467–4470.
(17) Rossi, R.; Carpita, A.; Bigelli, C. *Tetrahedron Lett.* **1985**, 523–526.

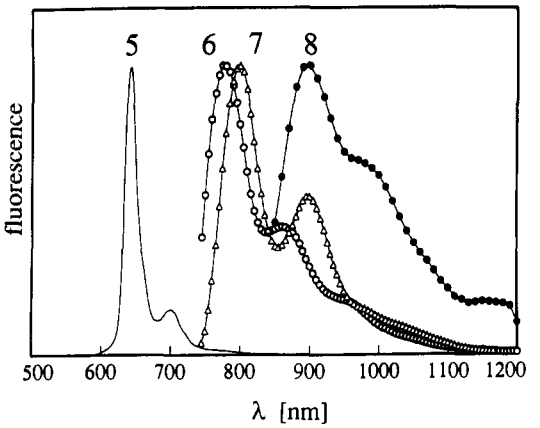

Figure 2. Normalized fluorescence spectra of 6.8 μM **6** (○), 5.3 μM **7** (△), and 14 μM **8** (●); the corrected fluorescence spectrum of **5** is given for comparison. All spectra in air-saturated benzene solutions. The spectra of **6** and **7** were recorded with a 455-nm cutoff filter in front of the cuvette and a 695-nm cutoff filter between the monochromator and the Ge detector. The corresponding filters in the case of **8** were for 530 and 850 nm.

benzene solutions of **6–8** are shown in Figure 2, together with the corrected emission spectrum of **5** for comparison purposes.

For the fluorescence lifetimes, τ_S, of **6** and **7** in degassed solutions see Table I. The values were distinctly lower in the presence of oxygen (data not quantified). The very long-wavelength range of the emission of **8** precluded a measurement of its τ_S.

Fluorescence Quantum Yields. The spectral range of fluorescence of the acetylene–cumulene porphyrinoids is red-shifted beyond the region where appropriate emission references are available. Conventional spectral integration for quantum yield determinations was therefore not possible, and steady-state thermal lensing was chosen instead. The method can be used to determine total luminescence. It detects irradiance changes of a CW laser beam passing through a solution, resulting from a change in refractive index by the heat evolving from radiationless transitions after light absorption.[19] Since none of the compounds unequivocally exhibited any phosphorescence in the range 900–1600 nm in degassed benzene and bromobenzene solutions at 293 K,[18] any contribution of phosphorescence to emission was neglected in the fluorescence measurements by thermal lensing,[19] viz., $\Phi_f \gg \Phi_p$. For the Φ_f values see Table I.

Irradiation Experiments. The ground-state absorption spectra of compounds **6** and **7** had not changed after 1000 laser shots had been fired in each case at both λ^{exc} values (640 and 720 nm) during the difference triplet–triplet (T–T[20]) absorption measurements (see Spectroscopic and Photochemical Methods for the corresponding laser fluence). A similar stability was exhibited by **8** at λ^{exc} = 532 nm. Any ΔA due to a photochemical change would therefore be $<10^{-3}$. The quantum yield for any photoreaction resulting in an absorption change should therefore be $<10^{-4}$ even if $\Delta\epsilon$ is assumed to be only 10^3 M^{-1} cm^{-1}.

The photostability of **6** was further confirmed by irradiation with λ^{exc} = 435 nm over extended periods in liquid 2-methyltetrahydrofuran solution at temperatures ranging from 302 to 193 K. Additional irradiation experiments were carried out with **6** and **7** in Ar matrices at 10 K with several λ^{exc} values from 253 nm to the far-red absorption region. In neither case could any photochemical change at the respective temperature be discerned by FTIR and UV–visible spectroscopy.

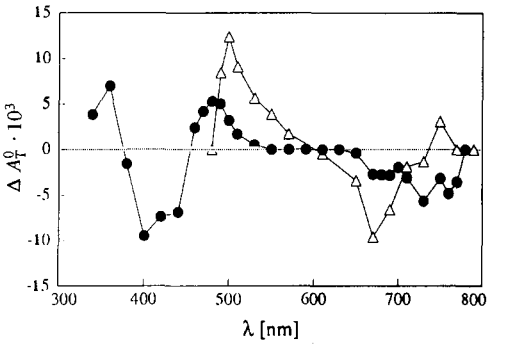

Figure 3. T–T absorption spectra of 11 μM **6** (●; λ^{exc} = 700 nm) and 29.5 μM **7** (△; λ^{exc} = 640 nm) in degassed benzene solutions.

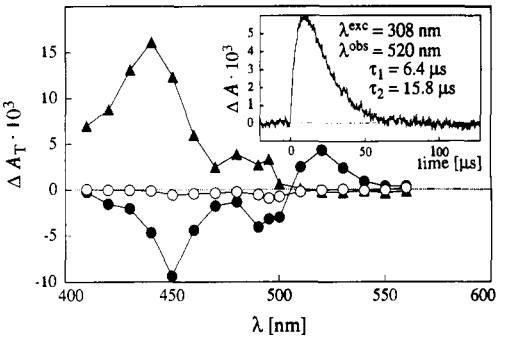

Figure 4. T–T absorption spectra of a benzene solution containing 0.4 mM acridine and 10.1 μM **8**; λ^{exc} = 308 nm. The spectra were recorded 0 μs (▲, showing the absorbance of triplet acridine), 20 μs (●, triplet **8**), and 200 μs (○, transient reaction product between triplet acridine and ground-state **8**) after the laser pulse. Inset: trace showing formation of triplet **8** (τ_1) and its decay (τ_2).

Table II. Rate Constants (k_q) for Quenching by Energy Transfer in Benzene at Room Temperature

donor	acceptor	k_q[a] (10^9 M^{-1} s^{-1})
triplet **6**	$O_2(^3\Sigma_g^-)$	0.09 ± 0.01
triplet **7**	**6**	1.79 ± 0.06
triplet **7**	$O_2(^3\Sigma_g^-)$	1.87 ± 0.09[b]
$O_2(^1\Delta_g)$	**7**	8.1 ± 2.8[b]
triplet **8**	$O_2(^3\Sigma_g^-)$	0.077[c]
triplet acridine	**8**	≤16[c]
triplet ZnTPP	**8**	5.2 ± 0.2
$O_2(^1\Delta_g)$	**8**	12 ± 1[d]

[a] The term k_q is used in this table as a general notation for the quenching constant. In the text a more explicit nomenclature serves to differentiate the individual values. [b] Values determined from reversible energy transfer. [c] Values determined from two acceptor concentrations. [d] Measured by time-resolved NIR phosphorescence detection.

Triplet State Properties. (a) T–T Absorption Spectra. The T–T absorption spectra of **6** and **7** are shown in Figure 3. The decay traces for both compounds were monoexponential with lifetimes of (90 ± 20) and (115 ± 28) μs, respectively.

(b) Energy Transfer to Compound 8 from Triplet Acridine. T–T absorption upon direct irradiation (λ^{exc} = 532 and 720 nm) of degassed benzene solutions of **8** could not be detected even at high laser fluence. However, the triplet state of **8** could be observed upon sensitization with acridine (λ^{exc} = 308 nm) under conditions where only 10% of the exciting light was absorbed by **8**. The absorption of triplet acridine, λ_{max} = 440 nm,[21a] decayed with a lifetime of (180 ± 7) μs in the absence of quencher. The absorbance changes after the laser pulse were monitored in the region λ^{obs} = 410–560 nm. The experimental traces were fitted to the sum of two exponential terms plus a constant according to eq 1, where a_1, a_2, and a_3 are constants for a given λ^{obs}, and τ_1 and τ_2

(18) Compound **7** exhibits some weak addition on the long-wavelength tail of fluorescence which appears to be phosphorescence on account of quenching by oxygen.

(19) (a) Negri, R. M.; Zalts, A.; San Román, E. A.; Aramendía, P. F.; Braslavsky, S. E. *Photochem. Photobiol.* **1991**, *53*, 317–322. (b) Nonell, S.; Aramendía, P. F.; Heihoff, K.; Negri, R. M.; Braslavsky, S. E. *J. Phys. Chem.* **1990**, *94*, 5879–5883.

(20) Abbreviations: LIOAS, laser-induced optoacoustic spectroscopy; T–T, difference triplet–triplet (absorption); ZnPC, dipyrtdyl complex of zinc(II) phthalocyanine; ZnTPP, zinc(II) tetraphenylporphyrin.

(21) (a) Carmichael, I.; Hug, G. L. *J. Phys. Chem. Ref. Data* **1986**, *15*, 36 and references therein, (b) 10, (c) 183.

are the decay lifetimes of the two components.

$$\Delta A = a_1 \exp(-t/\tau_1) + a_2 \exp(-t/\tau_2) + a_3 \quad (1)$$

The fitting function at zero time plotted for different observation wavelengths (see Figure 4) coincided with the T–T absorption spectrum of acridine.[21a] The energy-transfer rate constant from triplet acridine corresponded to a lifetime of (6.4 ± 1.4) μs, viz., the shorter lifetime component. From this value and the concentration of **8** a quenching constant of triplet acridine by **8** of 1.6×10^{10} M^{-1} s^{-1} is derived (Table II). The absorbance, derived from the fitting curve, at a time equal to about three lifetimes of triplet acridine (i.e., 20 μs after the laser pulse), is also shown in Figure 4.

The preexponential coefficient (a_2) of the longer lifetime, (15.8 ± 2.7) μs, was negative in the range 410–500 nm and positive between 510 and 560 nm. No signal was observed in the range 570–740 nm. Furthermore, at $\lambda^{obs} > 510$ nm, where triplet acridine does not absorb, the shorter lifetime, 6.4 μs, had a negative coefficient (see inset in Figure 4). This means that an absorbing species is formed from triplet acridine, with a risetime identical to the decay of triplet acridine (i.e., 6.4 μs). This species decays with a lifetime of 15.8 μs, and its absorption is observed at $\lambda^{obs} \geq 510$ nm. We assign this species to the triplet state of **8**.

The constant a_3 was obtained from fitting the traces during the first 200 μs after the laser pulse. It was negative in the range 410–560 nm. In order to measure the lifetime corresponding to the bleaching-recovery process responsible for a_3, the analyzing time range had to be extended. For this purpose, flash photolysis was performed without pulsing the analyzing lamp and without operating the shutter between this lamp and the sample. Under these conditions, a lifetime of (95 ± 3) ms was measured for the slow bleaching-recovery process. We propose a radical (ion) formed by reaction of triplet acridine with ground-state **8** to be the source of this slow bleaching and recovery. The assignment takes into consideration the use of a low-polarity solvent (benzene) and the long lifetime of the recovery at wavelengths where ground-state **8** absorbs. However, an absorption of any such radical has not been detected so far.

The error, introduced by the bleaching-recovery process in the spectrum taken 20 μs after the laser pulse, is negligible. Nevertheless, when this is taken into account the above-mentioned quenching constant of triplet acridine by **8** is an upper-limit value for the triplet–triplet energy-transfer process.

The ratio between the molar absorption coefficient maxima for the acceptor triplet **8** at 520 nm ($\Delta\epsilon_{T-T}^{520}$) and the donor triplet acridine at 440 nm ($\Delta\epsilon_{T-T}^{440}$) was calculated by eq 2.[21b,22]

$$\Delta\epsilon_{T-T}^{520}/\Delta\epsilon_{T-T}^{440} = (A^A/A^D)(k^D + k_q[\mathbf{8}] - k^A)/k_q[\mathbf{8}] \quad (2)$$

The absorbances of the donor at 440 nm (A^D) and of the acceptor at 520 nm (A^A) are values obtained by extrapolation to the end of the laser pulse. The rate constants k^D and k^A are for the decay of triplet acridine in the absence of **8** and for the decay of triplet **8**, respectively. Using $\Delta\epsilon_{T-T}^{440} = 2.5 \times 10^4$ M^{-1} cm^{-1},[21a] a value of $\Delta\epsilon_{T-T}^{520} = 2.4 \times 10^4$ M^{-1} cm^{-1} is calculated for triplet **8**.

(c) Energy Transfer to 8 from Triplet Zinc(II) Tetraphenylporphyrin (ZnTPP[20]). Flash photolysis of degassed benzene solutions of ZnTPP showed a monoexponential decay with a lifetime of (200 ± 4) μs. Experiments under the same conditions in the absence and in the presence of several concentrations of **8** afforded monoexponential decay kinetics, even at wavelengths where both triplet ZnTPP[21c] and triplet **8** (vide supra) absorb, e.g., at the maximum of T–T absorption of **8** (520 nm; see Figure 4). However, the lifetime of triplet ZnTPP (τ_T^D) decreased with increasing concentration of **8**, and $1/\tau_T^D$ was linearly dependent on [**8**]. The linear Stern–Volmer plot gave a rate constant of $k_q = 5.2 \times 10^9$ M^{-1} s^{-1} (Table II) for the quenching of triplet ZnTPP by **8**. This suggests that energy transfer from triplet ZnTPP to **8** occurs although the absorbance of triplet **8** was not observed.

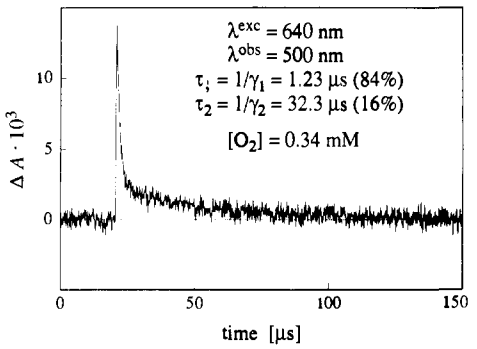

Figure 5. Biexponential triplet decay of **7** in benzene in the presence of O_2.

The decay lifetime in the solution of highest [**8**] (15.7 μM) was 11.6 μs. We attribute the apparent lack of a biexponential decay at 520 nm to the mathematical difficulty for the fitting program to discriminate two similar lifetimes, viz., the lifetimes of triplet **8** (15.8 μs; when sensitized by acridine, vide supra) and of triplet ZnTPP (11.6 μs). In the solutions containing **8** in *lower* concentrations, the decay of triplet **8** was overlapped by the decay of triplet ZnTPP yielding unreasonably long experimental lifetimes, viz., $1/k_{obs} \geq 38$ μs.

(d) Energy Transfer to 8 from Singlet Molecular Oxygen, $O_2(^1\Delta_g)$. When solutions of ZnTPP and **8** were saturated with air, the triplet state of **8** was detected in the range 450–550 nm. It was to be expected that under these conditions triplet ZnTPP should be quenched competitively by O_2 and **8**. In fact, from the concentrations ([O_2] = 2.2 mM;[23] [**8**] = 15.7 μM) and from the quenching constants of triplet ZnTPP by O_2, $k_q^{O_2} = 9.7 \times 10^9$ M^{-1} s^{-1},[24] and by **8**, $k_q = 5.2 \times 10^9$ M^{-1} s^{-1} (vide supra), values of $k_q^{O_2}[O_2] = 2.1 \times 10^6$ s^{-1} and $k_q[\mathbf{8}] \leq 8.2 \times 10^4$ s^{-1} can be calculated. The value of $k_q[\mathbf{8}]$ is thus 26 times smaller than that of $k_q^{O_2}[O_2]$, and 99.8% of the triplet states of ZnTPP should be trapped by oxygen in air-saturated benzene. This then suggests that triplet **8** in the above experiment was formed predominantly by energy transfer from $O_2(^1\Delta_g)$ to ground-state **8**.

The experimental decays of the T–T absorption in the range 450–550 nm were fitted to the sum of two monoexponential terms, with no constant term being necessary in this case. The fitting function 3 μs after the laser pulse, which contained mostly the longer decay lifetime (4.3 ± 0.5) μs, had the same shape as the T–T absorption spectrum of **8** shown in Figure 4.

A quenching constant of triplet **8** by O_2 of 7.7×10^7 M^{-1} s^{-1} is derived from the triplet lifetimes of **8** in degassed (15.8 μs, from the above experiments with acridine as triplet sensitizer) and in air-saturated solutions (4.3 μs).

Measurement by time-resolved detection of NIR phosphorescence from $O_2(^1\Delta_g)$ of the quenching by **8**, in an experiment using ZnTPP as the sensitizer, gave a linear Stern–Volmer plot, which afforded a rate constant of 1.2×10^{10} M^{-1} s^{-1} (Table II). This diffusional value supports the postulate (vide supra) that energy transfer from $O_2(^1\Delta_g)$ generated the triplet state of **8**.

Determination of $\Phi_T^0\,\Delta\epsilon_{T-T}$. The zero time absorbances at the wavelengths of the T–T absorption maxima of **5** (reference), **6**, and **7** were linear functions of the laser pulse energy, E_{laser}.

Using the literature data for **5** [$\Phi_T^0 = 0.4 \pm 0.1$ and $\Delta\epsilon_{T-T}^{395} = (2.1 \pm 0.6) \times 10^4$ M^{-1} cm^{-1}],[19] the slopes of the straight lines gave $\Phi_T^0\,\Delta\epsilon_{T-T}$ values (at 480 and 500 nm) of $(4.3 \pm 1.6) \times 10^3$ and $(1.1 \pm 0.1) \times 10^4$ M^{-1} cm^{-1} for **6** and **7**, respectively.

Triplet Energy Transfer from Compound 7. (a) To Molecular Ground-State Oxygen. The triplet state of **7** decayed biexponentially in the presence of $O_2(^3\Sigma_g^-)$ (Figure 5). This behavior is due to reversible energy transfer between $O_2(^3\Sigma_g^-)$ and triplet states close in energy to $O_2(^1\Delta_g)$. It has already been observed for some naphthalocyanines[25a,b] and phthalocyanines.[25c] Analogous

(22) Braslavsky, S. E.; Schneider, D.; Heihoff, K.; Nonell, S.; Aramendía, P. F.; Schaffner, K. *J. Am. Chem. Soc.* **1991**, *113*, 7322–7334.

(23) *Solubilities of Inorganic and Organic Compounds*; Stephen, H., Stephen, T., Eds.; Macmillan: New York, 1963; Vol. 1, p 573.

(24) Ganzha, V. A.; Gurinovich, G. P.; Egorova, G. D.; Sagun, E. I.; Shul'ga, A. M. *Zh. Prikl. Spektrosk.* **1989**, *50*, 618.

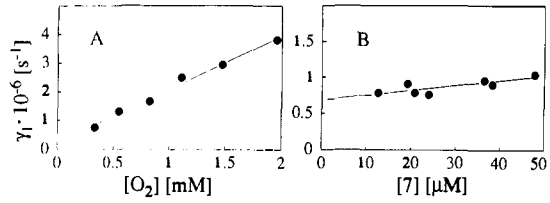

Figure 6. Determination of k_f and k_r in benzene: dependence of γ_1 on the concentrations of O_2 (A) and **7** (B).

to the interpretation of these cases,[25] eq 3 is proposed to account for the biexponential decay of triplet **7** (=^{3}**7**).

$$^3\mathbf{7} + O_2(^3\Sigma_g^-) \underset{k_r}{\overset{k_f}{\rightleftharpoons}} \mathbf{7} + O_2(^1\Delta_g) \qquad (3)$$

^{3}**7** → **7** (k_T); $O_2(^1\Delta_g)$ → $O_2(^3\Sigma_g^-)$ (k_Δ)

According to this model, the shorter lifetime component (rate constant γ_1) is expected to be given by eq 4 under the condition that $k_f[O_2(^3\Sigma_g^-)] \gg k_T$ and $k_r[7] \gg k_\Delta$.

$$\gamma_1 = k_f[O_2] + k_r[7] \qquad (4)$$

In order to obtain the k_f and k_r values, [7] was kept constant (22.6 μM) at various [O_2]. The slope of the straight line of γ_1 vs [O_2] (Figure 6A) gave $k_f = 1.87 \times 10^9$ M^{-1} s^{-1} (Table II), and the intercept $k_r[7]$ afforded $k_r = (9.7 \pm 4.4) \times 10^9$ M^{-1} s^{-1}. An independent value for k_r was obtained from measurements of γ_1 at constant [O_2] = 0.34 mM and variable [7] (Figure 6B). The values thus obtained are $k_r = 8.1 \times 10^9$ M^{-1} s^{-1} (Table II) and $k_f = (1.85 \pm 0.26) \times 10^9$ M^{-1} s^{-1}. They are within the error limits the same as the corresponding values from Figure 6A. Finally, from k_f and k_r an equilibrium constant of $K = k_f/k_r = 0.23$ is calculated.

The longer decay component (rate constant γ_2) of triplet **7** corresponds to the lifetime of $O_2(^1\Delta_g)$ in benzene. The value of $1/\gamma_2 = (33 \pm 5)$ μs (average of several measurements) agrees with literature data.[26]

The plots (not shown) of $O_2(^1\Delta_g)$ phosphorescence intensity at zero time, I_0, as a function of $E_{laser}(1 - 10^{-A})$ upon excitation of **7** at 355 and 666 nm in air-saturated benzene solution were linear. Compounds **5** ($\Phi_\Delta = 0.36 \pm 0.05$[19b]) and the dipyridyl complex of zinc(II) phthalocyanine (ZnPC;[28] $\Phi_\Delta = 0.50 \pm 0.06$[27]), respectively, served as references. The $O_2(^1\Delta_g)$ lifetime of (30 ± 4) μs in these experiments at both excitation wavelengths was as reported[26] for benzene solutions. The slopes for **7** afforded Φ_Δ values of an average 0.06 (Table I).

Of course the biexponential nature of the ^{3}**7** decay requires that the $O_2(^1\Delta_g)$ phosphorescence decay is biexponential. However, the time resolution of our detection system (ca. 3 μs) precluded the recording of the short lifetime component.

No $O_2(^1\Delta_g)$ phosphorescence was observed in air-saturated benzene solutions of **6** (λ^{exc} = 355 and 640 nm) and of **8** (λ^{exc} = 720 nm).

(b) Triplet Energy Transfer from 7 to 6. Flash photolyses of degassed benzene solutions containing both **6** and **7** were carried out at λ^{exc} = 800 nm where the ground-state absorbance of **7** is 10 times larger than that of **6** at its highest concentration (for the absorption spectra, see Figure 1). The decay kinetics of triplet **7** was monoexponential at λ^{obs} = 560 nm where triplet **6** does not absorb, and the decay was biexponential at wavelengths where both triplets absorb. The decay lifetime of triplet **7** (λ^{obs} = 560 nm) decreased with increasing concentration of **6**. The linear Stern–Volmer plot (not shown) gave a rate constant of 1.79×10^9 M^{-1} s^{-1} for the quenching of triplet **7** by ground-state **6** (Table II).

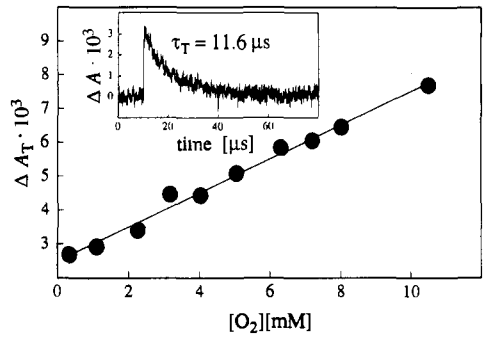

Figure 7. O_2-induced enhancement of singlet → triplet intersystem crossing in **6**: transient absorbance at zero time, ΔA_T vs O_2 concentration in benzene. Inset: triplet decay of **6** in the presence of 1.1 mM O_2; λ^{obs} = 480 nm.

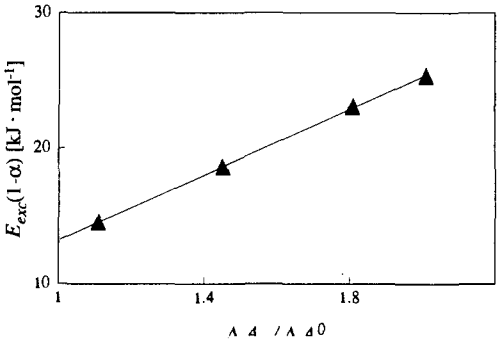

Figure 8. Determination by LIOAS of $\Phi_T^0 E_T$ and $\Phi_f(E_f)$: plot of $E^{exc}(1 - \alpha)$ vs $\Delta A_T/\Delta A_T^0$ for **6** in the presence of 0.5–4 mM O_2;[39] λ^{exc} = 700 nm, τ'_a = 229 ns.

Effects of Molecular Ground-State Oxygen and Bromobenzene on the Excited States of Compound 6. Triplet **6** decayed monoexponentially in solutions containing O_2 in concentrations ranging from zero to saturation. A linear Stern–Volmer plot (not shown) of the first-order rate constant, k^{obs} vs [O_2], afforded a rate constant for the quenching of **6** by O_2 of $k_q^{O_2} = 9 \times 10^7$ M^{-1} s^{-1} (Table II).

The presence of O_2 in solutions of **6** led not only to quenching of the triplet state but also to enhanced S → T intersystem crossing, as indicated by an increase in triplet state absorption at zero time after the laser pulse. In order to quantify this effect by O_2 the ΔA_T value, extrapolated to zero time, is plotted vs [O_2] in Figure 7. In the presence of O_2 the intersystem crossing quantum yield, Φ_T, increases by a factor of 3 upon O_2 saturation of an initially degassed solution of **6**.

The addition of bromobenzene to **6** resulted in a linear increase in ΔA_T. At a concentration of 1.9 M bromobenzene ΔA_T was 2.4 times the value in neat benzene. The effect is paralleled by a decrease in fluorescence. This fluorescence quenching can be described by the Medinger–Wilkinson equation (eq 5)[28] which assumes that bromobenzene converts all otherwise emitting excited singlet-state molecules to triplets. I_0 and I are the fluorescence

$$I_0/I = [(I_0\Delta A_T/I\Delta A_T^0) - 1]\Phi_T^0 + 1 \qquad (5)$$

intensities with and without the added fluorescence quencher bromobenzene. The plot of I_0/I vs $(I_0\Delta A/I\Delta A_0) - 1$ (not shown) affords an intercept of 0.98 ± 0.02 and a slope (Φ_T^0, in neat benzene) of 0.16 ± 0.02 (Table I).

This method assumes that bromobenzene does not affect the internal conversion yield. In fact, optoacoustic measurements with **6** in benzene as a function of bromobenzene concentration (0–5

(25) (a) Firey, P. A.; Ford, W. E.; Sounik, J. R.; Kenney, M. E.; Rodgers, M. A. J. *J. Am. Chem. Soc.* **1988**, *110*, 7626–7630. (b) Ford, W. E.; Rihter, B. D.; Rodgers, M. A. J. *J. Am. Chem. Soc.* **1989**, *111*, 2362–2363. (c) Rihter, B. D.; Kenney, M. E.; Ford, W. E.; Rodgers, M. A. J. *J. Am. Chem. Soc.* **1990**, *112*, 8064–8070.

(26) Hurst, J. R.; McDonald, J. D.; Schuster, G. B. *J. Am. Chem. Soc.* **1982**, *104*, 2065–2067.

(27) Nonell, S. Ph.D. Thesis, MPI Strahlenchemie/Institut Quimic de Sarriá, Barcelona, 1988.

(28) Medinger, T.; Wilkinson, F. *Trans. Faraday Soc.* **1965**, *61*, 620–630.

M) gave $\alpha = 0.95 \pm 0.05$ (equal to internal conversion yield, see the following paragraph), without any concentration trend. The Φ_T^0 is therefore correct within the experimental error. As shown below, the value of $\Phi_T^0 E_T$ is derived from the correlation of the optoacoustic and flash photolysis data obtained in the absence and presence of O_2, implying that O_2 affects the internal conversion yield. The two experiments appear contradictory at first sight. However, the α value on closer inspection dropped with increasing O_2 concentration from 0.93 to 0.85 (Figure 8). The variation brought about by bromobenzene is smaller and therefore not detected within the experimental error of the photocalorimetric method.

Laser-Induced Optoacoustic Spectroscopy. The heat stored by triplet **7**, $\Phi_T^0 E_T$, in degassed solution was determined by LIOAS.[20] The amplitude of the first signal deflection H is related to the laser pulse energy, E_{laser}, and to A by eq 6,[19,29,30]

$$H = K\alpha E_{laser}(1 - 10^{-A}) \quad (6)$$

in which K is a proportionality constant involving geometrical parameters and thermoelastic properties of the solvent, and α is the fraction of absorbed energy dissipated as heat within the effective acoustic time, τ'_a.

In order to determine the α value of **7**, H vs E_{laser} was monitored at $\tau'_a = 760$ ns for degassed benzene solutions of both **7** and a calorimetric reference, I_2, with various absorbances at λ^{exc}. The ratio of the slopes of the straight lines obtained for H/E_{laser} plotted vs $(1 - 10^{-A})$ yields an α value of 0.83.

A value of $\Phi_T^0 E_T = 20.2$ kJ·mol^{-1} (Table I) was obtained from the energy balance equation (eq 7),

$$E^{exc}(1 - \alpha) = \Phi_f^0\langle E_f\rangle + \Phi_T^0 E_T \quad (7)$$

where E^{exc} is the excitation energy per mole of photons, $\langle E_f\rangle$ the mean fluorescence energy, and E_T the triplet energy.

A similar energy balance accounts for the results of the LIOAS experiments with **6** in the presence of O_2 (eq 8),

$$E^{exc}(1 - \alpha) = \Phi_f\langle E_f\rangle + \Phi_T E_T \quad (8)$$

where Φ_T denotes a value corresponding to a particular concentration of O_2. Since in the case of **6** ΔA_T increases linearly with $[O_2]$ (Figure 7), Φ_T can be expressed by eq 9 in terms of Φ_T^0 and ΔA_T^0, the corresponding values in the absence of O_2.

$$\Phi_T = \Phi_T^0(\Delta A_T/\Delta A_T^0) \quad (9)$$

Substitution of Φ_T in eq 8 by eq 9 predicts a linear relationship between $E^{exc}(1 - \alpha)$ and $\Delta A_T/\Delta A_T^0$, with a slope of $\Phi_T^0 E_T$, which was borne out by experiment: The α values were again observed from the ratio of the slopes of H/E_{laser} plots for benzene solutions of **6** and I_2 of matched absorbances at $\lambda^{exc} = 700$ nm. In Figure 8 the values of $E^{exc}(1 - \alpha)$ at various O_2 concentrations are plotted vs $\Delta A_T/\Delta A_T^0$. These latter ratios were obtained by flash photolysis at the corresponding O_2 concentrations. The $[O_2]$ range for these experiments was chosen such that the lifetime of triplet **6** in the solution with the highest $[O_2]$ was >1 μs and therefore $\gg\tau'_a$ = 229 ns. The slope in Figure 8 is $\Phi_T^0 E_T = 12.2$ kJ·mol^{-1} (Table I), and the intercept in the absence of oxygen, i.e., at $\Delta A_T/\Delta A_T^0 = 1$, is $\Phi_f^0\langle E_f\rangle + \Phi_T^0 E_T = (13 \pm 2)$ kJ·mol^{-1}.[31]

Determination of Triplet Energies, Quantum Yields of S → T Intersystem Crossing, and Triplet Absorption Coefficients. The combination of results affords values of E_T, Φ_T^0, and $\Delta\epsilon_{T-T}$ (Table I) as follows. For **6**, the values of $\Phi_T^0 = 0.16$ (from eq 5) and $\Phi_T^0 E_T = 12.2$ kJ·mol^{-1} (from LIOAS at various $[O_2]$) afford $E_T = 78$ kJ·mol^{-1}, and Φ_T^0 and $\Phi_T^0 \Delta\epsilon_{T-T}^{480} = 4.4 \times 10^3$ M^{-1} cm^{-1} (from the comparative method) give $\Delta\epsilon_{T-T}^{480} = 2.7 \times 10^4$ M^{-1} cm^{-1}.

From $k_f/k_r = 0.23$ at 293 K a $\Delta G°$ value of 3.6 kJ·mol^{-1} is derived for the reversible energy transfer between **7** and O_2. Since $\Delta G° = E_\Delta - E_T$ (neglecting entropic factors) and $E_\Delta = 94.4$ kJ·mol^{-1} [which is the energy required to promote $O_2(^3\Sigma_g^-)$ to $O_2(^1\Delta_g)$[32]], an E_T value of 91 kJ·mol^{-1} is obtained for **7**. Using $\Phi_T^0 E_T = 20.2$ kJ·mol^{-1} (from LIOAS), then, affords a value of 0.22 for Φ_T^0, and Φ_T^0 and $\Phi_T^0 \Delta\epsilon_{T-T}^{500} = 1.1 \times 10^4$ M^{-1} cm^{-1} (from the comparative method) lead to $\Delta\epsilon_{T-T}^{500} = 5 \times 10^4$ M^{-1} cm^{-1}.

No absorption of triplet **8** in 12 μM degassed benzene solution could be detected at $\lambda^{obs} = 520$ nm, even at saturating laser pulse energy (31 mJ at $\lambda^{exc} = 532$ nm). With $\Delta\epsilon_{T-T}^{520} = 2.4 \times 10^4$ M^{-1} cm^{-1} (from energy transfer from triplet acridine) and a detection limit of $\Delta A_T^0 < 5 \times 10^{-4}$, the concentration of any triplet **8** formed under these conditions should be $<2 \times 10^{-8}$ M, and Φ_T^0 should be $< 2 \times 10^{-3}$.

Discussion

All rate constants for quenching by energy transfer measured in the present work are compiled in Table II.

The diffusion-controlled rate constant for $O_2(^1\Delta_g)$ quenching by **8** and the observation of triplet **8** thereby generated document that this energy transfer is an efficient process.[33] The triplet energy of **8** is therefore at least 12 kJ·mol^{-1} below E_Δ, i.e., $E_T^8 <$ 82 kJ·mol^{-1}.

The quenching of triplet ZnTPP ($E_T = 155$ kJ·mol^{-1} [34]) by **8** is clearly slower than diffusion controlled, although the T–T energy gap would be sufficiently large (>73.5 kJ·mol^{-1}). Steric hindrance of the energy transfer is a possible explanation[35] for this finding. The quenching of triplet **7** by **6** occurs also more slowly by 1 order of magnitude than under diffusion control. Although the process is exothermic by a mere 12 kJ·mol^{-1}, the clean monoexponential decay even at $\lambda^{obs} = 560$ nm, where only triplet **7** absorbs, rules out any important contribution by a reversible energy transfer. Again, we prefer to assign the relatively low quenching rate constant to steric factors due to the bulkiness of the two molecules.

The Interactions of Compounds 6–8 with Molecular Oxygen. The quenching rate constants of the triplet states of **6** and **8** by O_2 [(8–9) × 10^7 M^{-1} s^{-1}] are lower than all other values published for this constant. Since no $O_2(^1\Delta_g)$ was detected in the case of **6**, we attribute the value for this compound to the low triplet energy which impairs the generation of $O_2(^1\Delta_g)$ by triplet quenching. In spite of the low Φ_T^0 value for **8**, the same argument can be applied for this compound due to the fact that the reverse energy transfer, i.e., from $O_2(^1\Delta_g)$ to ground-state **8**, shows a diffusionally controlled rate constant. Therefore, the dissociation of a singlet encounter complex of aromatic triplet and $O_2(^3\Sigma_g^-)$ to aromatic ground state and $O_2(^1\Delta_g)$ can be ruled out for both compounds, and the quenching is only due to the dissociation of triplet encounter complex to aromatic ground state and $O_2(^3\Sigma_g^-)$ (enhanced T → S intersystem crossing).[36]

The fact that $\Phi_\Delta < \Phi_T$ for **7** in both air- and O_2-saturated solutions indicates that in the quenching of its triplet state by $O_2(^3\Sigma_g^-)$ the dissociation to products of both singlet and triplet encounter complexes takes place.[37] Should all the quenching events be due to the dissociation of the singlet complex, then Φ_Δ should equal Φ_T at every oxygen concentration. Under such conditions, the term $RT \ln (1/9)$,[25] arising from the spin-statistical

(29) Patel, C. K.; Tam, A. C. *Rev. Mod. Phys.* **1981**, *53*, 517–550.
(30) Heihoff, K.; Braslavsky, S. E. *Chem. Phys. Lett.* **1986**, *131*, 183–188. Braslavsky, S. E.; Heihoff, K. In *Handbook of Organic Photochemistry*; Scaiano, J. C., Ed.; CRC Press: Boca Raton, 1989; pp 327–356. Braslavsky, S. E.; Heibel, G. E. *Chem. Rev.* **1992**, *92*, 1381–1410.
(31) Note that the product $\Phi_f\langle E_f\rangle$ changes with the oxygen concentration. However, since the value is a mere 10% of the slope, such changes will have only little effects on the deviation from linearity in Figure 8.
(32) Kasha, M. In *Singlet O$_2$*; Frimer, A. A., Ed.; CRC Press: Boca Raton, 1988; Vol. 1, pp 1–12.
(33) Lamola, A. A. In *Energy Transfer and Organic Photochemistry*; Lamola, A. A., Turro, N. J., Eds.; Wiley-Interscience: New York, 1969; pp 17–132.
(34) Harriman, A. *J. Chem. Soc., Faraday Trans. 2* **1981**, *77*, 1281–1291.
(35) Scaiano, J. C.; Leigh, W. J.; Meador, M. A.; Wagner, P. J. *J. Am. Chem. Soc.* **1985**, *107*, 5806–5807.
(36) Aromatic triplet state molecules and $O_2(^3\Sigma_g^-)$ form encounter pairs with quintet, triplet, and singlet multiplicities (Saltiel, J.; Atwater, B. W. In *Advances in Photochemistry*; Volman, D. H., Hammond, G. S., Gollnick, K., Eds.; Wiley: New York, 1988; Vol. 14, pp 1–90). The dissociation of the quintet complex does not lead to products, while the triplet complex yields $O_2(^3\Sigma_g^-)$ and ground-state sensitizer, and the singlet complex affords $O_2(^1\Delta_g)$ and ground-state sensitizer.
(37) Redmond, R. W.; Braslavsky, S. E. *Chem. Phys. Lett.* **1988**, *148*, 523–529.

factor $^1/_9$ in k_f, should be used to correct $\Delta G°$, which would affect the resulting E_T. This is not the case for **7** since both singlet and triplet complexes dissociate to products. Thus, the correction in $\Delta G°$ should be $RT \ln (^4/_9) = 2$ kJ·mol^{-1}, which is much smaller than the error limits for E_T.

Fluorescence quenching by $O_2(^3\Sigma_g^-)$ can result in $O_2(^1\Delta_g)$ generation only if the energy gap between the singlet and triplet states, ΔE_{S-T}, is greater than E_Δ.[38] This energetic requirement is not fulfilled by **7** ($\Delta\epsilon_{S-T}$ ca. 58 kJ·mol^{-1}). Therefore, the generation of $O_2(^1\Delta_g)$ from singlet-excited **7** is energetically unfavorable.

For **6** (τ_S = 1.0 ns; E_S = 153 kJ·mol^{-1}) the lack of $O_2(^1\Delta_g)$ generation by quenching of either the singlet or triplet states implies 60 kJ·mol^{-1} < E_T < 94.4 kJ·mol^{-1}, in good agreement with the value resulting from LIOAS in combination with the Φ_T^0 value (E_T = 78 kJ·mol^{-1}; cf. Table I).

The estimated internal conversion quantum yields for **6** and **7** are Φ_{ic}^0 = 0.91 and 0.79, respectively (Table I). These values (both compounds have 22 conjugated π electrons) are much higher than those for free-base porphyrins[39] and porphycenes[19] (18π systems; Φ_{ic} in the range 0.2–0.3), and they are in the range of the value for a 26π porphyrin [Φ_{ic} = 0.83, as calculated from $1 - (\Phi_f + \Phi_T)$].[40] Since the tendency of Φ_{ic} to increase with the number of π conjugated electrons is accompanied by a decrease in the energy of the singlet-excited state, this is in agreement with a dependence of the Franck–Condon overlap on E_S.[41]

The contributions of the diverse deactivation channels of the excited acetylene–cumulene porphyrinoids are summarized in Table I. The Φ_{ic}^0, Φ_f, and Φ_T^0 values of **5**, **6**, and **7** add up close to unity within a relatively large overall experimental error. In the 26π compound **8** deactivation is restricted essentially to internal conversion. The lack of any observable unimolecular photoreactivity, even at low temperature, is particularly noteworthy in the case of triplet **7**, which, e.g., should have lesser conformational constraints toward *E,Z* isomerization than triplet **5**[42] and **6**. The preferential accepting modes for internal conversion of **5–8** therefore appear to involve rotations around the single bonds of the substituents and/or concerted N–H proton shifts.

Conclusion. None of **6–8** exhibit any phosphorescence,[18] so that other ways had to be chosen for the triplet energy determination of these compounds. While E_T of **7** was determined by reversible energy transfer to $O_2(^3\Sigma_g^-)$,[25] new strategies had to be employed for **6** and **8**. Indirect detection by LIOAS of the increase in triplet yield induced by $O_2(^3\Sigma_g^-)$-enhanced S → T intersystem crossing afforded the E_T of **6**. Although the Φ_T^0 values for both **6** and **7** are near 0.2, the lower triplet energy of **6** (E_T = 78 kJ·mol^{-1} < E_Δ) precludes $O_2(^1\Delta_g)$ generation by this compound.

The small triplet quantum yield for **8** ($\Phi_T^0 < 2 \times 10^{-3}$) in solution did not allow the observation of its triplet state by direct irradiation and rendered the determination of its triplet state properties difficult; nevertheless, an upper limit of E_T could be obtained by energy-transfer experiments from $O_2(^1\Delta_g)$ to **8**.

The 22π and 26π homologous porphyrinoids **6–8** attracted our attention also in view of our previous evaluation of the porphycenes **1** and **5** as potential sensitizers in photodynamic therapy.[2] Both fully meet a priori criteria[43]—under in-vitro conditions in liquid solution[2a] and unilamellar lipid vesicles,[2b,44] as well as in in-vivo tests with mice,[45]—defined as prerequisites for dyes to qualify as agents suited for photodynamic tumor localization and therapy. Thus, both **1** and **5** are well-defined homogeneous substances, their absorption above 630 nm is quite intense (e.g., see Figure 1), they are highly photostable, and they possess relatively high quantum yields for fluorescence, S → T intersystem crossing, and photosensitized formation of $O_2(^1\Delta_g)$ in homogeneous liquid solution[2a] and lipid vesicles.[2b,44] Moreover, pharmacokinetic investigations have shown that **5** is localized with high selectivity in tumors of mice and efficiently destroys the malignant tissue upon red-light irradiation.[45]

In preliminary phototherapeutic tests[46] compound **7** has now also been found to be a potential candidate for tumor localization and phototherapy when incorporated into unilamellar liposomes and administered by intravenous injection to mice bearing transplated fibrosarcoma. The results compare favorably with the corresponding performance of the parent porphycene **5**,[45] and we should note that **7** has the additional advantage of a considerably farther red-shifted and more intense absorption.[47] The appreciably lower Φ_Δ values for **7** (Φ_Δ = 0.06 vs 0.36 for **5**[2a,19]) thus does not appear to diminish critically its role as a photodynamic sensitizer. In contrast, compounds **6** and **8**—both with negligible sensitizer activities if any at all ($\Phi_\Delta < 10^{-3}$)—failed to have any phototherapeutic effect under similar conditions.[46] This finding constitutes an interesting example where in a homologous series of dyes the failure to meet one of the a priori criteria [viz., in-vitro formation of $O_2(^1\Delta_g)$][48] suffices to block any phototherapeutic activity.

Experimental Section

Synthesis of the 26π Porphyrinoid 8: General Procedures. Melting points were measured on a Reichert Thermovar and are uncorrected. ^{1}H and ^{13}C NMR spectra were recorded on a Bruker AM 300 spectrometer. Chemical shifts are expressed in parts per million downfield from internal TMS (δ). Electronic absorption spectra of the compounds mentioned in this section were recorded on a Perkin-Elmer Lambda 7 UV–visible spectrophotometer. Mass spectra were obtained on Finnigan 3200 and Varian MAT 212 instruments, and IR spectra were taken on a Perkin-Elmer 1600 Series FTIR spectrophotometer. Elemental analyses were performed by Bayer AG, Leverkusen, Germany.

3,4-Diethyl-2-formyl-5-[(trimethylsilyl)ethynyl]pyrrole (10). To a solution of **9**[8] (5.54 g, 20 mmol) in diethylamine (200 mL) were added under argon (trimethylsilyl)acetylene (3 g, 30 mmol), bis(triphenylphosphine)palladium(II) chloride (0.25 g, 0.36 mmol), and copper(I) iodide (0.13 g, 0.7 mmol). The homogeneous mixture was stirred at 50 °C for 30 min. After evaporation of the solvent in vacuo, the residue was subjected to chromatography on a short silica gel column (length 15 cm, diameter 2 cm) with ether/pentane (1:3) as the eluent to give **10** (4.44 g, 90%) which was pure by NMR and was used directly. An analytical sample was obtained by recrystallization from *n*-hexane as slightly yellow needles: mp 71–72 °C; ^{1}H NMR (300 MHz, $CDCl_3$) δ 9.56 (s, 1 H), 8.99 (br s, 1 H), 2.68 (q, J = 7.6 Hz, 2 H), 2.49 (q, J = 7.6 Hz, 2 H), 1.19 (t, J = 7.6 Hz, 3 H), 1.15 (t, J = 7.6 Hz, 3 H), 0.23 (s, 9 H); ^{13}C NMR (75.5 MHz, $CDCl_3$) δ 177.01, 136.04, 132.46, 128.42, 118.43, 102.37, 95.09, 17.72, 17.34, 16.97, 14.97, –0.26; MS (EI, 70 eV) m/z 247 (M^+, 97), 232 (100), 174 (37), 73 (59); IR (KBr) 3247, 2963, 2153, 1644, 1447, 1384, 1244, 883, 842, 760, 733, 639 cm^{-1}; UV–visible ($C-H_2Cl_2$) λ_{max} [nm] (ϵ) = 240 (12000), 332 (27100). Anal. Calcd for $C_{14}H_{21}NOSi$: C, 67.96; H, 8.56; N, 5.66. Found: C, 67.64; H, 8.06; N, 5.50.

5-Ethynyl-3,4-diethyl-2-formylpyrrole (11). A solution of **10** (5 g, 20 mmol) in methanol (125 mL) was treated with a 1 N aqueous solution of sodium hydroxide (125 mL) whereby heat was evolved. The resulting mixture was stirred for 30 min and then treated with a solution of ammonium chloride (7.5 g) in water (125 mL). Water was then added until **11** had precipitated completely. After filtration and thorough washing with water and drying (magnesium sulfate), **11** was recrystallized from *n*-hexane to give yellowish plates (3.19 g, 90%): mp 108–110 °C; ^{1}H NMR (300 MHz, $CDCl_3$) δ 9.58 (s, 1 H), 9.44 (br s, 1 H), 3.42 (s, 1 H), 2.70 (q, J = 7.6 Hz, 2 H), 2.51 (q, J = 7.6 Hz, 2 H), 1.20 (t, J = 7.6 Hz, 3 H), 1.14 (t, J = 7.6 Hz, 3 H); ^{13}C NMR (75.5 MHz, $CDCl_3$)

(38) McLean, A. J.; McGarvey, D. J.; Truscott, T. G.; Lambert, C. R.; Land, E. J. *J. Chem. Soc., Faraday Trans. 2* **1990**, *86*, 3075–3080.
(39) Seybold, P. G.; Gouterman, N. *J. Mol. Spectrosc.* **1969**, *31*, 1–13.
(40) Schermann, G.; Schmidt, R.; Völcker, A.; Brauer, H.-D.; Mertes, H.; Franck, B. *Photochem. Photobiol.* **1990**, *52*, 741–744.
(41) Turro, N. J. *Modern Molecular Photochemistry*; Benjamin/Cummings Publishing Company: Menlo Park, 1978; p 183.
(42) Compound **5** proved equally photostable in previous irradiation experiments.[2a]
(43) van den Bergh, H. *Chem. Br.* **1986**, *22*, 430–439.
(44) Nonell, S.; Braslavsky, S. E.; Schaffner, K. *Photochem. Photobiol.* **1990**, *51*, 551–556.
(45) Guardiano, M.; Biolo, R.; Jori, G.; Schaffner, K. *Cancer Lett.* **1989**, *44*, 1–6. Milanesi, C.; Biolo, R.; Jori, G.; Schaffner, K. *Lasers Med. Sci.* **1991**, *6*, 437–442.
(46) Unpublished results by G. Jori and collaborators.
(47) The farther red-shifted and more intense absorption of the exciting light provides for greater penetration into the tissue and higher phototherapeutic efficacy upon administration of substantially lower photosensitization doses. This should reduce the risk of systemic toxicity of the photosensttization in the absence of irradiation.
(48) Cf.: Moan, J. J. *J. Photochem. Photobiol. B* **1990**, *5*, 521–524.

δ 177.28, 136.22, 132.67, 128.62, 117.52, 83.97, 74.51, 17.58, 17.37, 16.95, 15.20; MS (EI, 70 eV) *m/z* 175 (M^+, 100), 160 (98), 117 (36); IR (KBr) 3261, 3211, 2964, 2106, 1621, 1441, 1383, 1336, 1235, 753 cm^{-1}; UV-visible (CH_2Cl_2) λ_{max} [nm] (ε) = 233 (9600), 321 (21 600). Anal. Calcd for $C_{11}H_{13}NO$: C, 75.40; H, 7.48; N, 7.99. Found: C, 75.15; H, 7.49; N, 7.69.

1,4-Bis(3,4-diethyl-5-formyl-2-pyrryl)butadiyne (12). A mixture of **11** (1.75 g, 10 mmol) and chloroacetone (0.93 g, 10 mmol) in dry benzene (50 mL) was added to a solution of tetrakis(triphenylphosphine)palladium(0) (0.23 g, 0.2 mmol), copper(I) iodide (0.14 g, 0.75 mmol), and triethylamine (2.0 g, 20 mmol) in dry benzene (50 mL). After stirring the reaction mixture at room temperature for 16 h, the solvent was removed in vacuo, and the residue, dissolved in hot ethyl acetate, was passed through a short silica gel column. Extraction of the silica gel with hot ethyl acetate was continued until the product (yellow fluorescence) was eluted. Recrystallization of the product from ethyl acetate afforded pure (by ^1H NMR) **12** (1.30 g, 75%). An analytical sample was obtained by an additional recrystallization [from ethanol/ethyl acetate (1:1)] as yellow needles (dec >210 °C): ^1H NMR (300 MHz, [D_5]pyridine) δ 14.10 (br s, 1 H), 9.95 (s, 1 H), 2.70 (q, *J* = 7.6 Hz, 2 H), 2.57 (q, *J* = 7.6 Hz, 2 H), 1.19 (t, *J* = 7.6 Hz, 3 H), 1.16 (t, *J* = 7.6 Hz, 3 H); ^{13}C NMR (75.5 MHz, [D_5]pyridine) δ 178.25, 135.44, 134.79, 131.21, 116.78, 79.91, 77.21, 18.15, 17.44, 17.25, 15.86; MS (EI, 70 eV) *m/z* 348 (M^+, 100), 277 (27), 174 (8); IR (KBr) 3238, 2966, 1627, 1441, 1376, 1232 cm^{-1}; UV-visible (CH_2Cl_2) λ_{max} [nm] (ε) = 227 (20 700), 269 (17 100), 361 (38 500), 380 (42 100), 411 (38 200). Anal. Calcd for $C_{22}H_{24}N_2O_2$: C, 75.83; H, 6.94; N, 8.04. Found: C, 75.44; H, 7.01; N, 7.86.

2,3,10,11,16,17,24,25-Octaethyl-5,6,7,8,19,20,21,22-octadehydro[26]-porphyrin-(2.4.2.4) (8). A slurry of activated zinc (1.31 g, 20 mmol), copper(I) chloride (0.14 g, 1.4 mmol), and dry tetrahydrofuran (100 mL) in an oven-dried flask was treated dropwise with freshly distilled titanium tetrachloride (1.89 g, 10 mmol) under argon. The mixture was then heated with stirring at reflux temperature for 3 h. A solution of **12** (0.35 g, 1.0 mmol) in tetrahydrofuran (80 mL) was then added slowly at reflux. After heating for another 10 min, the reaction mixture was allowed to cool and then quenched by addition of a half-concentrated aqueous solution of ammonia (50 mL). Subsequently, chloroform was added and the inorganic material was separated by filtration through celite. The aqueous phase was extracted with chloroform, and the combined organic phases were washed with water and dried over magnesium sulfate. Concentration in vacuo afforded a black residue which was chromatographed on a silica gel column (length 15 cm, diameter 5 cm) using carbon disulfide as the eluent. Recrystallization of the product from dichloromethane/hexane (1:1) gave compound **8** as green rhombs with metallic luster (27 mg, 9%); dec >260 °C: ^1H NMR (300 MHz, CS_2/CD_2Cl_2) δ 10.08 (s, *J* = 7.6 Hz, 4 H), 4.63 (q, *J* = 7.6 Hz, 8 H), 4.22 (q, *J* = 7.6 Hz, 8 H), 2.41 (t, *J* = 7.6 Hz, 12 H), 2.09 (t, *J* = 7.6 Hz, 12 H), 2.04 (br s, 2 H); ^{13}C NMR (75.5 MHz, CS_2/CD_2Cl_2) δ 144.04, 143.47, 141.36, 127.18, 113.05, 95.84, 94.82, 22.04, 21.04, 19.33, 18.53; MS (EI, 70 eV) *m/z* 630 (M^+, 100), 315 (5); *m/z* calcd (M^+) for $C_{44}H_{46}N_4$ 630.3722, obsd 630.3647; IR (CsI) 2965, 2931, 2869, 2022, 1479, 1304, 1261, 1201, 1149, 1111, 1054, 998, 945 cm^{-1}; UV-visible (CH_2Cl_2) λ_{max} [nm] (ε) = 285 (18 000) sh, 240 (14 100), 391 (24 800) sh, 423 (61 100) sh, 448 (158 000), 495 (103 400), 753 (19 400) sh, 792 (42 900) sh, 804 (45 400) sh, 839 (98 300), 889 (119 600); (C_6H_6) 450 (123 000), see Figure 1. Anal. Calcd for $C_{44}H_{46}N_4$: C, 83.77; H, 7.35; N, 8.88. Found: C, 83.69; H, 7.29; N, 8.64.

Single-crystal X-ray analysis of **8**: Crystals from benzene, dec >260 °C; triclinic, space group $P\bar{1}$, *Z* = 1, *a* = 8.514 (2), *b* = 8.837 (2), *c* = 13.305 (4) Å, α = 105.47 (2), β = 106.72 (2), γ = 95.45 (2)°; ρ_{calcd} = 1.154 g·cm^{-1}; intensities measured on an Enraf Nonius CAD-4 diffractometer [room temperature, λ_{Mo} = 0.71069 Å, Θ_{Mo}(max) = 25°]; refinement (C and N anisotropic, H isotropic) taking into consideration 1718 reflections with $F_o > 4\,\sigma(F_o)$; R = 0.051, R_w = 0.052. For further details of the crystal structure investigation see supplementary material.

Photophysical and Photochemical Study: Materials. Benzene, bromobenzene, and pyridine used for measurements were spectroscopic grade (Merck, Uvasol). ZnTPP was prepared as described.[49] Zn(II) phthalocyanine from CIBA-Geigy (Basel) was used as received, elemental and spectroscopic analyses being satisfactory.[50] Acridine (96%, Ega Chemie) was recrystallized.[51] The laser dyes DCM (640 nm), Pyridine-1 (700 nm), and Styril-9 (800 nm) were used as received from Radiant Dyes Chemie (Wermelskirchen).

Spectroscopic and Photochemical Methods (for further details see also Table I). The benzene solutions of the samples were deaerated by either flushing with Ar or degassing in five freeze–pump(<10^{-1} Pa)–thaw cycles. UV-visible absorption spectra for the photophysical investigation were measured with a Cary 17 spectrophotometer, and FTIR spectra were recorded with a Perkin-Elmer M1760 spectrometer.

Steady-state fluorescence of several air-saturated 12 μM solutions of **6** containing 0–1.9 M bromobenzene was recorded at room temperature with a computer-controlled Spex Fluorolog instrument; λ^{exc} = 680 nm, λ^{em} = 770 nm.

Steady-State NIR Luminescence. In the home-built emission spectrophotometer[19b] the excitation light from a 2500-W Xe lamp was filtered by 3 cm of water, two KG-5 filters, and a cutoff filter (Schott, Mainz). Another cutoff filter was placed between monochromator and Ge detector. Emission spectra were recorded at room temperature.

Fluorescence quantum yields (Φ_f) for **6–8** were determined at 293 K by steady-state thermal lensing as described previously,[19] except that for **8** an Ar ion CW laser (514 nm, 0.5 mW; Spectra Physics) beam was focused on the cuvette by means of an 8-cm convergent lens. *meso*-Tetraphenylporphyrin, prepared and purified as published,[52] was used as a calorimetric reference. The instrumentation was similar to that described by Magde et al.[53] Compounds **6** and **7** in Ar-flushed benzene solutions were excited with a 1-mW He–Ne laser (Melles-Griot) at 633 nm. Absorbances at 633 nm (for **6** and **7**) and 514 nm (for **8**) were determined on a Cary 2300 spectrophotometer with a precision of 0.0003 AU. No spectral changes were observed after these irradiations.

Singlet excited state lifetimes (τ_S) of **6** and **7** were measured in degassed solutions with a single-photon-counting fluorimeter. For details of the instrumental set-up and the mathematical algorithm for the data handling see refs 54 and 55, respectively.

Triplet measurements by flash photolysis were carried out with improved versions of systems described previously,[56,57] exciting either with a Q-switched Nd:YAG laser (System 2000, J. K. Lasers; pulse width 15 ns) operating at the second harmonics (λ^{exc} = 532 nm) or with a dye laser [pumped with the second harmonics of the Nd:YAG laser or a XeCl excimer laser (Lambda Physik, Göttingen; pulse width 15 ns, λ^{exc} = 308 nm)].

T–T absorption spectra of **6** and **7** were obtained by excitation at 700 and 640 nm, respectively (laser fluences = 5–6 mJ·cm^{-2}).

Flash photolysis experiments with **8** were performed in degassed benzene solution. Laser fluences were up to 2 mJ·cm^{-2} at λ^{exc} = 720 nm, and up to 31 mJ·cm^{-2} at 532 nm; A = 0.12 at both λ^{exc} values.

The T–T absorption spectrum of **8** was measured by the energy-transfer method in two series of experiments: (i) solutions of 0.4 mM acridine (A_{308} = 0.82) without and with **8** (10 μM) at λ^{exc} = 308 nm; (ii) solutions of ZnTPP (A_{532} = 0.20) without and with several concentrations of **8** (up to 15.7 μM) at λ^{exc} = 532 nm. In series i degassed solutions were analyzed, while in series ii both degassed and air-saturated solutions were employed. In both series, the laser pulse energy, E_{laser}, was chosen such that the sensitizer triplet decay in the quencher-free solution was monoexponential.

For the measurement of the S → T intersystem crossing quantum yield (Φ_T^0), the comparative method of Bensasson[58] was employed to determine $\Phi_T^0\,\Delta\epsilon_{T-T}$ values in degassed benzene solutions. The dependence of the zero time absorbance on laser energy was determined at λ^{exc} = 640 nm and λ^{obs} = 480 (**6**) and 500 nm (**7**); the reference was **5**, $\Phi_T^0\,\Delta\epsilon_{T-T}^{395} = 8400\ M^{-1}\ cm^{-1}$.[19b] Absorbances of ca. 0.27 of samples and references were matched at λ^{exc}. Laser fluences (<2 mJ·cm^{-2}) were chosen such that the extrapolation of the decay trace to time zero, ΔA_T^0, was proportional to the fluence.

The effect of molecular ground-state oxygen on the triplet-state kinetics was analyzed by monitoring the triplet decays of **6** (λ^{exc} = 700 nm, λ^{obs} = 480 nm, laser fluence = 2 mJ·cm^{-2}) and **7** (λ^{exc} = 640 nm, λ^{obs} = 500 nm, laser fluence = 5 mJ·cm^{-2}) in benzene as a function of O_2

(49) Rossbroich, G.; García, N. A.; Braslavsky, S. E. *J. Photochem.* **1985**, *31*, 37–47.
(50) Valduga, G.; Reddi, E.; Jori, G. *J. Inorg. Biochem.* **1987**, *29*, 59–65.
(51) Wolf, A. P.; Anderson, R. C. *J. Am. Chem. Soc.* **1955**, *77*, 1608–1612.
(52) Adler, A. D.; Longo, F. R.; Finarelli, J. D.; Goldmacher, J.; Assour, J.; Korsakoff, L. *J. Org. Chem.* **1967**, *32*, 476. Barnett, G. H.; Hudson, M. F.; Smith, K. M. *J. Chem. Soc., Perkin Trans. 1* **1975**, 1401–1403.
(53) Magde, D.; Brannon, J. H.; Cremers, T. L.; Olmsted, J., III. *J. Phys. Chem.* **1979**, *83*, 696–699.
(54) Matthews, J. I.; Braslavsky, S. E.; Camillert, P. *Photochem. Photobiol.* **1980**, *32*, 733–738.
(55) Wendler, J.; Holzwarth, A. R.; Braslavsky, S. E.; Schaffner, K. *Biochim. Biophys. Acta* **1984**, *786*, 213–221.
(56) Aramendia, P. F.; Ruzsicka, B. P.; Braslavsky, S. E.; Schaffner, K. *Biochemistry* **1987**, *26*, 1418–1422. Krieg, M.; Aramendia, P. F.; Braslavsky, S. E.; Schaffner, K. *Photochem. Photobiol.* **1988**, *47*, 305–310.
(57) Ruzsicska, B. P.; Braslavsky, S. E.; Schaffner, K. *Photochem. Photobiol.* **1985**, *41*, 681–688.
(58) Bensasson, R. V.; Goldschmidt, C. R.; Land, E. J.; Truscott, T. G. *Photochem. Photobiol.* **1978**, *28*, 277–281.

concentration. For this purpose, an O_2/N_2 mixture (gas mixer: Brooks Instruments Division, Hatfield, PA) was bubbled into the solution, and the O_2 concentration was calculated using Henry's law and 2.2 mM as the O_2 concentration in air-saturated benzene.[23]

The amount of triplet **6** produced at λ^{exc} = 700 nm and laser fluence = 4.3 mJ·cm^{-2} in 12 μM benzene solutions with 0–1.9 M bromobenzene was estimated from the ΔA_T value extrapolated to zero time.

The rate constant of quenching of triplet **7** by **6** was determined from the triplet decay of 12 μM **7** in degassed solutions with 0–49 μM **6**.

In **laser-induced optoacoustic spectroscopy (LIOAS)**[30] N_2-saturated benzene solutions, with A_{640} = 0.04–0.16, of **7** and of a calorimetric reference, I_2,[59] were excited by a dye laser (λ^{exc} = 640 nm). The effective acoustic transit time, τ'_a, was 760 ns, and the laser fluence was kept below 15 μJ. In experiments with **6** (λ^{exc} = 700 nm), the dependence of the signal amplitude on the O_2 concentration was analyzed. An air-saturated solution of I_2 (A_{700} = 0.205) was used as the reference, τ'_a was 229 ns, and the laser energies were below 2 μJ. For the adjustment of ground-state oxygen concentrations in the solution of **6** (A_{700} = 0.205) vide supra.

The instrumental set-up for the time-resolved NIR phosphorescence detection from $O_2(^1\Delta_g)$ has already been described.[60] The solutions were excited either at 355 nm (Nd:YAG frequency-tripled) or at 666 nm (DCM pumped by the second harmonics of the Nd:YAG laser). The emission was monitored at λ > 1050 nm (silicon cutoff filter, Glen Creston, thickness 2 mm); its decay in air-saturated benzene solutions of **7** was biexponential. The shorter-lifetime term, with a time constant of <3 μs, was due to the response of the detector to fast sample fluorescence and light scattering. The longer-lifetime term was the $O_2(^1\Delta_g)$ phosphorescence and yielded the $O_2(^1\Delta_g)$ lifetime in benzene.

Quantum yields of $O_2(^1\Delta_g)$ formation, Φ_Δ, in benzene were obtained by the comparative method[27] from the amplitude of the longer-lived signal extrapolated back to zero time, I_0. Air-saturated benzene solutions of **5** (Φ_Δ = 0.36 ± 0.05[2a,t9b]) and ZnPC dipyridyl complex (Φ_Δ = 0.50 ± 0.06[27]) were used as references at λ^{exc} = 355 and 666 nm, respectively. The laser fluence was <1.3 mJ·cm^{-2}.

The rate constant for the quenching of $O_2(^1\Delta_g)$ by **8** was determined by conventional Stern–Volmer experiments[60] using ZnTPP (A_{532} = 0.4) as a sensitizer in air-saturated solutions. The laser fluence (λ^{exc} = 532 nm) was <0.2 mJ·cm^{-2}. An additional band-pass filter at 1270 nm (Spectrogon) reduced the strong fluorescence before reaching the detector.

Steady-state irradiations (light source: 1000-W Hg–Xe lamp with monochromator, bandwidth 13–14 nm) were carried out (i) with 2-methyltetrahydrofuran solutions of **7** (A_{790} ca. 0.07, 10^{-5} M) at several temperatures from 302 to 193 K (λ^{exc} = 435 nm) (see Results, Irradiation Experiments, for further experiments in liquid solution at room temperatures) and (ii) with **6** (sublimation at 493 K) and **7** (sublimation at 473 K) in Ar matrices at 10 K [several λ^{exc} values from >695 nm (cutoff filter) to 253 nm; for a description of the matrix isolation set-up see ref 61]. Product analysis was performed with FTIR and UV–visible absorption spectroscopy.

Acknowledgment. P.F.A. is a member of Carrera del Investigador; R.M.N. and D.O.M. (in part) have been supported by the Consejo Nacional de Investigaciones Científicas y Técnicas (CONICET) of Argentina and N. J. by the Fonds der Chemischen Industrie (Stiftung Stipendienfonds). Private communications by Professor G. Jori, University of Padua, are gratefully acknowledged. We thank Dr. R. Scurlock for valuable discussions, Dr. W. E. Klotzbücher and G. Klihm for the low-temperature irradiation experiments, S. Griebenow, E. Hüttel, A. Keil, and G. Koç-Weier for technical assistance, and E. Rodriguez-Val for preparing octaethyl[22]porphyrin-(2.2.2.2). The Bundesministerium für Forschung und Technologie (Verbundstudie "Photodynamische Lasertherapie"), the Deutsche Forschungsgemeinschaft, the Volkswagen-Stiftung (all Fed. Rep. Germany), and the CONICET (PIA E 0919/87) supported parts of this work.

Supplementary Material Available: For **8**, tables of detailed information on the crystal structure determinations, final atomic position parameters, final thermal parameters, and interatomic distances and angles (8 pages); listing of observed and calculated structure factors (13 pages). Ordering information is given on any current masthead page.

(59) Tam, A. C.; Patel, C. K. N.; Kerl, R. J. *Opt. Lett.* **1979**, *4*, 81.
(60) Valduga, G.; Nonell, S.; Reddi, E.; Jori, G.; Braslavsky, S. E. *Photochem. Photobiol.* **1988**, *48*, 1–5.
(61) Gerhartz, W.; Grevels, F.-W.; Klotzbücher, W. E. *Organometallics* **1987**, *6*, 1850–1856. Klotzbücher, W. E. *Cryogenics* **1983**, *23*, 554–556.

Electron-Transfer Quenching of Excited Diphenylmethyl Radicals[1]

Bradley R. Arnold,*,† J. C. Scaiano,*,†,[2] and W. G. McGimpsey*,‡

Contribution from the Steacie Institute for Molecular Sciences, National Research Council, Ottawa, Canada K1A 0R6, and Department of Chemistry, Worcester Polytechnic Institute, Worcester, Massachusetts 01609. *Received May 19, 1992*

Abstract: The intermolecular reactivity of the excited diphenylmethyl radical (DPM*) has been studied with particular emphasis on electron-transfer reactions. These studies allow the determination of the rate constants for the reaction of DPM* with electron acceptors. For example, carbon tetrachloride, methyl benzoate, and benzyl bromide quench DPM* with rate constants of 3.3 × 10^8, 1 × 10^6, and 3.6 × 10^6 M^{-1} s^{-1} in acetonitrile. The corresponding carbocation is an observable product of the reaction, leaving no doubt that the reaction involves electron transfer. A kinetic salt effect is observed for the reaction of DPM* with carbon tetrachloride, where the carbocation yield increases from ca. 61% to ca. 100% with the addition of small concentrations of tetrabutylammonium perchlorate. The lower limits to the rates of back electron transfer (BET) and ion pair escape (ESC) for the product cation and radical anions in acetonitrile solution have been estimated using reductive dehalogenation of aryl halides as clock reactions where the rates of fragmentation have been estimated.

Introduction

There are very few studies of intermolecular reactions of excited organic free radicals,[3-10] particularly when compared to the volumes of data reported for other excited states. This observation may be attributed to two factors. First, the ground-state reactivity of most organic free radicals is quite high under normal conditions

† Steacie Institute for Molecular Sciences.
‡ Worcester Polytechnic Institute.

(1) Issued as NRCC-33326.
(2) Present address; Department of Chemistry, University of Ottawa, Ottawa, Ontario, Canada K1N 6N5.
(3) Fox, M. A.; Gaillard, E.; Chen, C.-C. *J. Am. Chem. Soc.* **1987**, *109*, 7088.

0002-7863/92/1514-9978$03.00/0